Optical Engineering

SPIEDigitalLibrary.org/oe

Mechanically compensated type for midwave infrared zoom system with a large zoom ratio

Zhou Hao
Liu Ying
Sun Qiang
Li Chun
Zhang Xiaolong
Huang Jianbo

Mechanically compensated type for midwave infrared zoom system with a large zoom ratio

Zhou Hao
Chinese Academy of Sciences
Changchun Institute of Optics
Fine Mechanics, and Physics
Changchun 130033, China
and
Graduate School of the Chinese Academy of Sciences
Beijing 100049, China
E-mail: ciompzh@hotmail.com

Liu Ying
Sun Qiang
Li Chun
Chinese Academy of Sciences
Changchun Institute of Optics
Fine Mechanics, and Physics
Changchun 130033, China

Zhang Xiaolong
Chinese Academy of Sciences
Changchun Institute of Optics
Fine Mechanics, and Physics
Changchun 130033, China
and
Graduate School of the Chinese Academy of Sciences
Beijing 100049, China

Huang Jianbo
Chinese Academy of Sciences
Changchun Institute of Optics
Fine Mechanics, and Physics
Changchun 130033, China

Abstract. In some circumstances, there is a need for a midwave infrared (MWIR) zoom system with a large zoom ratio. Using traditional four-component mechanically compensated types of MWIR zoom systems cannot achieve a large zoom ratio. To meet this demand, we describe a six-component mechanically compensated type. The thin-lens theory of this type is developed and equations are presented. Using the six-component mechanically compensated type, a MWIR continuous zoom system with a zoom ratio of 45 is designed, and it has high image quality over the entire zoom range. [DOI: 10.1117/1.OE.52.1.013002]

Subject terms: midwave infrared; continuous zoom; large zoom ratio; optical design.

Paper 121531 received Oct. 22, 2012; revised manuscript received Nov. 23, 2012; accepted for publication Dec. 4, 2012; published online Jan. 7, 2013.

1 Introduction

Infrared systems operating in midwave infrared (MWIR, from 3 to 5 μm) are used in civilian and military applications, such as law enforcement, life rescue, territorial surveillance, vehicle tracking, aerial surveillance, and stealth searching.[1–3] In recent years, the demand for MWIR zoom systems has increased. In these systems, the wide field of view (WFOV) is used for observing a large scene area for possible targets of interest, and the narrow field of view (NFOV) is used for close-up identification of the target of interest.[3–12] In some circumstances, such as aerial surveillance and life rescue, there is a need for wider observation of the scene.[3] There is a significant need to design a MWIR zoom system with a large zoom ratio.

There are two types of zoom systems: optically compensated and mechanically compensated. Almost all infrared zoom systems are mechanically compensated.[13] In a traditional mechanically compensated zoom system, the second component moves for changes in focal length, while the third component moves to eliminate image shift; the image stays in focus throughout the zoom range (refer to Fig. 1).[13] Using a traditional four-component mechanically compensated type, MWIR zoom systems cannot achieve a large zoom ratio (such as 45) with a general F/number (such as 4).[1,2,14–21] In this paper, we examine the six-component mechanically compensated type, which can achieve a large zoom ratio. The design concept is shown in Fig. 2; the second and fourth components are linked and move together for changes in focal length, while the third and fifth components are linked and move together to eliminate image shift. This type still involves just two moving groups. It is likely that the zoom range could also be achieved with a third moving group, but there is additional expense and complexity to do so. Section 2 presents the thin-lens theory. In Sec. 3, a MWIR continuous zoom system with a zoom ratio of 45 is designed. Finally, in Sec. 4, we present our conclusions.

2 Thin-Lens Theory

Figure 3 represents a general six-component zoom system, with the zoom components in their long-zoom positions.

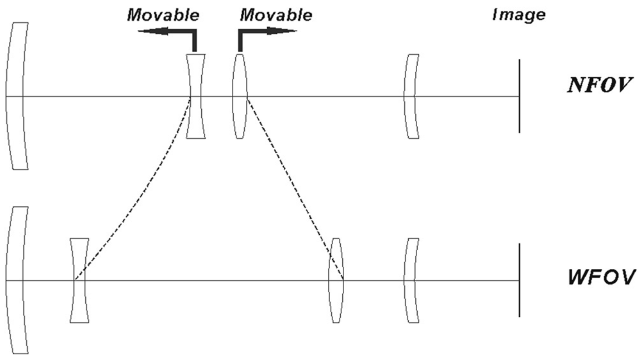

Fig. 1 Four-component mechanically compensated zoom system.

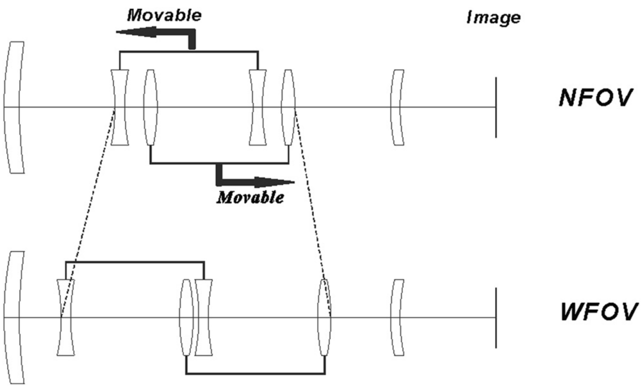

Fig. 2 Six-component mechanically compensated zoom system.

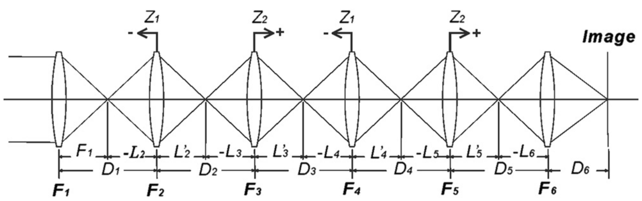

Fig. 3 General six-component zoom system.

Capital letters indicate the long-zoom values. Thin-lens theory is used to investigate the zooming properties. For the second component,

$$\frac{1}{L_2'}-\frac{1}{L_2}=\frac{1}{F_2}, \tag{1}$$

where F_2 is the focal length of the component.

This becomes

$$L_2'=\frac{F_2\cdot L_2}{F_2+L_2}, \tag{2}$$

and

$$L_2=F_1-D_1. \tag{3}$$

Likewise, for the third component,

$$L_3'=\frac{F_3\cdot L_3}{F_3+L_3}, \tag{4}$$

but

$$L_3=L_2'-D_2. \tag{5}$$

For the fifth component,

$$\frac{1}{L_5'}-\frac{1}{L_5}=\frac{1}{F_5}. \tag{6}$$

This becomes

$$L_5=\frac{F_5\cdot L_5'}{F_5-L_5'}, \tag{7}$$

and

$$L_5'=D_5+L_6. \tag{8}$$

Likewise for the sixth component,

$$L_6=\frac{F_6\cdot D_6}{F_6-D_6}. \tag{9}$$

Likewise, for the fourth component,

$$L_4=\frac{F_4\cdot L_4'}{F_4-L_4'}, \tag{10}$$

but

$$L_4'=D_4+L_5, \tag{11}$$

and

$$L_3'-L_4=D_3. \tag{12}$$

Therefore, using Eqs. (2)–(5) and (7)–(11) in Eq. (12),

$$\frac{F_3\cdot\left[\frac{F_2\cdot(F_1-D_1)}{F_2+F_1-D_1}-D_2\right]}{F_3+\frac{F_2\cdot(F_1-D_1)}{F_2+F_1-D_1}-D_2}-\frac{F_4\cdot\left[D_4+\frac{F_5\cdot\left(D_5+\frac{F_6\cdot D_6}{F_6-D_6}\right)}{F_5-D_5-\frac{F_6\cdot D_6}{F_6-D_6}}\right]}{F_4-D_4-\frac{F_5\cdot\left(D_5+\frac{F_6\cdot D_6}{F_6-D_6}\right)}{F_5-D_5-\frac{F_6\cdot D_6}{F_6-D_6}}}=D_3. \tag{13}$$

As the second, third, fourth, and fifth components move from their long-zoom positions, the image should stay in focus, and the following conditions must hold:

$$\frac{F_3\cdot\left[\frac{F_2\cdot(F_1-d_1)}{F_2+F_1-d_1}-d_2\right]}{F_3+\frac{F_2\cdot(F_1-d_1)}{F_2+F_1-d_1}-d_2}-\frac{F_4\cdot\left[d_4+\frac{F_5\cdot\left(d_5+\frac{F_6\cdot d_6}{F_6-d_6}\right)}{F_5-d_5-\frac{F_6\cdot d_6}{F_6-d_6}}\right]}{F_4-d_4-\frac{F_5\cdot\left(d_5+\frac{F_6\cdot d_6}{F_6-d_6}\right)}{F_5-d_5-\frac{F_6\cdot d_6}{F_6-d_6}}}=d_3. \tag{14}$$

Small letters indicate the values at the new zoom position. As previously defined, Z_1 is the axial distance moved by the second and fourth components from the long-zoom position, and Z_2 is the axial distance moved by the third and fifth components at zoom setting Z_1 from the long-zoom position. Thus,

$$d_1 = D_1 + Z_1. \tag{15}$$

$$d_2 = D_2 + Z_2 - Z_1. \tag{16}$$

$$d_3 = D_3 - Z_2 + Z_1. \tag{17}$$

$$d_4 = D_4 + Z_2 - Z_1. \tag{18}$$

$$d_5 = D_5 - Z_2. \tag{19}$$

$$d_6 = D_6. \tag{20}$$

And by combining Eqs. (14)–(20),

$$Z_2 + \frac{a_1 \cdot Z_2^2 + b_1 \cdot Z_2 + c_1}{Z_2^2 - b_2 \cdot Z_2 - c_2} + \frac{b_3 \cdot Z_2 - 2}{Z_2 - c_4} - c_5 = 0, \tag{21}$$

where

$$a_1 = F_4$$

$$b_1 = F_4 \cdot \left(D_4 - D_5 - \frac{F_6 \cdot D_6}{F_6 - D_6} - Z_1\right),$$

$$b_2 = F_4 - D_4 + Z_1 + D_5 + \frac{F_6 \cdot D_6}{F_6 - D_6}$$

$$b_3 = F_3$$

$$c_1 = F_4 \cdot \left(F_5 - D_5 - \frac{F_6 \cdot D_6}{F_6 - D_6}\right) \cdot (D_4 - Z_1) + F_4 \cdot F_5 \cdot \left(D_5 + \frac{F_6 \cdot D_6}{F_6 - D_6}\right)$$

$$c_2 = \left(F_5 - D_5 - \frac{F_6 \cdot D_6}{F_6 - D_6}\right) \cdot (F_4 - D_4 + Z_1) - F_5 \cdot \left(D_5 + \frac{F_6 \cdot D_6}{F_6 - D_6}\right)$$

$$c_3 = F_3 \cdot \left[\frac{F_2 \cdot (F_1 - D_1 - Z_1)}{F_2 + F_1 - D_1 - Z_1} - D_2 + Z_1\right]$$

$$c_4 = F_3 + \frac{F_2 \cdot (F_1 - D_1 - Z_1)}{F_2 + F_1 - D_1 - Z_1} - D_2 + Z_1$$

$$c_5 = D_3 + Z_1$$

At the zoom setting Z_1, as the long-zoom values are known, the above values of a_1, b_1, b_2, b_3, c_1, c_2, c_3, c_4 and c_5 can then be evaluated. After rearrangement, Eq. (21) becomes

$$Z_2^4 + k_3 \cdot Z_2^3 + k_2 \cdot Z_2^2 + k_1 \cdot Z_2 + k_0 = 0, \tag{22}$$

where

$$k_3 = a_1 - b_2 + b_3 - c_4 - c_5$$

$$k_2 = b_1 - c_2 - c_3 - a_1 \cdot c_4 - b_2 \cdot b_3 + b_2 \cdot c_4 + b_2 \cdot c_5 + c_4 \cdot c_5$$

$$k_1 = c_1 - b_1 \cdot c_4 + b_2 \cdot c_3 - c_2 \cdot b_3 + c_2 \cdot c_4 + c_2 \cdot c_5 - b_2 \cdot c_4 \cdot c_5$$

$$k_0 = -c_1 \cdot c_4 + c_2 \cdot c_3 - c_2 \cdot c_4 \cdot c_5$$

Using Eq. (22), the motion of the third and fifth components Z_2 at the the zoom setting Z_1 may be evaluated. Using Eqs. (14)–(19), the distance values may be found. Then, the

Table 1 Characteristics of the system.

Zoom range	45
Focal length range	−10 to −450 mm
F/number	4
Image plane diagonal	12 mm
Spectral band	3.7 to 4.8 μm

Table 2 The initial data of the thin-lens zoom system.

F_1	135.646	D_1	79.188
F_2	−36.930	D_2	9.528
F_3	71.126	D_3	105.237
F_4	−38.214	D_4	15.312
F_5	50.702	D_5	172.529
F_6	27.052	D_6	51.512

NOTE: Unit: mm.

corresponding effective focal length (EFL) of the system is obtained.

3 Example of the Design

A MWIR zoom system designed with a 320×240 staring focal plane array, and the dimension of detector pixel is $30 \times 30\ \mu m^2$. The characteristics of the design are shown in Table 1.

Table 3 Thin-lens data of the system at three zoom positions.

	Long EFL	Mid EFL	Short EFL
Z_1	0	−17.121	−53.587
Z_2	0	30.708	43.004
d_1	79.188	62.067	25.601
d_2	9.528	57.357	106.119
d_3	105.237	57.408	8.646
d_4	15.312	63.141	111.903
d_5	172.529	141.821	129.525
d_6	51.512	51.512	51.512
EFL	−450	−63.2	−10

NOTE: Unit: mm.

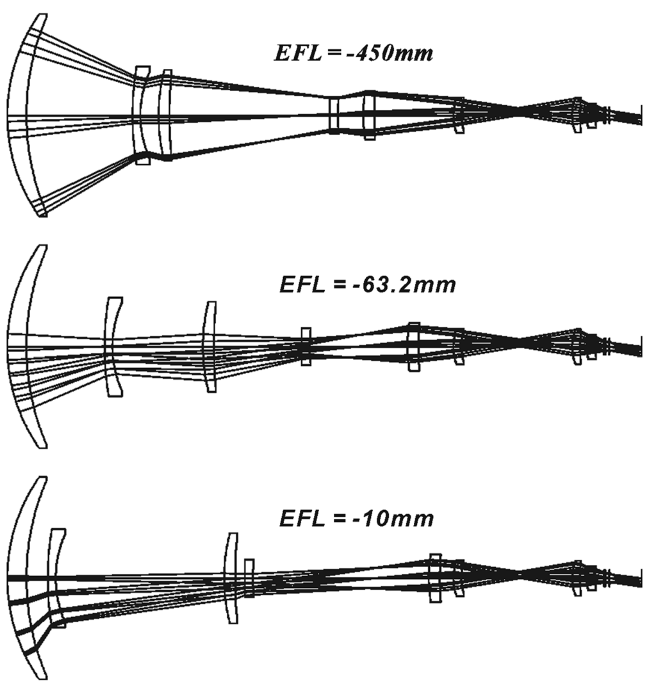

Fig. 4 Layouts of the actual system at three zoom positions.

3.1 *Thin-Lens Results*

The initial data of the thin-lens system at the long-zoom position (EFL = −450 mm) are listed in Table 2. Using Eqs. (22) and (14)–(19), setting three different values of Z_1, thin-lens data of the system at the three zoom positions are calculated and listed in Table 3.

3.2 *Actual Results*

According to the thin-lens design results, the original structure of the actual system was obtained. Computer optimization was initiated at three zoom positions and was expanded to nine and eventually to 34 zoom positions. The actual zoom system consists of eight elements, made from silicon and germanium to achieve achromatization. There are four aspheric surfaces utilized for compactness in order to achieve the desired optical performance. Layouts of the system at three zoom positions are shown in Fig. 4. Characteristics of the system are shown in Table 1. The overall length of the zoom system is 400 mm. The second and fourth elements are linked and move together; the length of the move is 53.45 mm over the entire zoom range. The third and fifth elements are also linked and move together; the length of the move is 41.40 mm over the entire zoom range. The overall length and moving lengths are short compared with those of the typical zoom systems.[1,15] Figure 5 shows the continuous motions of the zoom elements; the focal length of the system is smooth and continuous. To have 100% cold shielding efficiency, the cold shield of the detector and the exit pupil of the system have to be superposed.

3.3 *Performance*

The modulation transfer function (MTF) performances of the system at three zoom positions are shown in Fig. 6. The MTF value in Nyquist limit ($16l$ p/mm) is more than 0.3 over the entire zoom range. Figure 7 illustrates spot diagrams for three different zoom positions. Root mean square (RMS) radius of the spot is less than 30 μm over the full zoom range. The MWIR zoom system has high image quality.

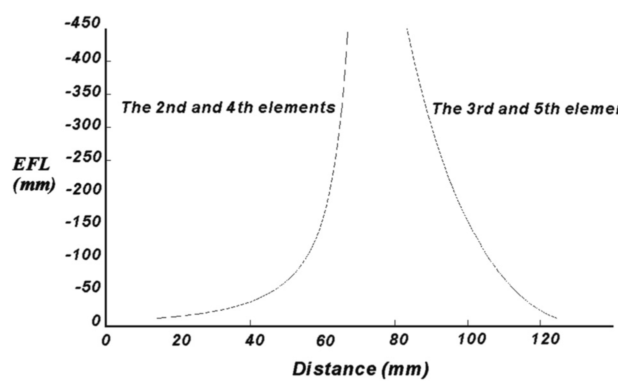

Fig. 5 The zoom paths of the actual system.

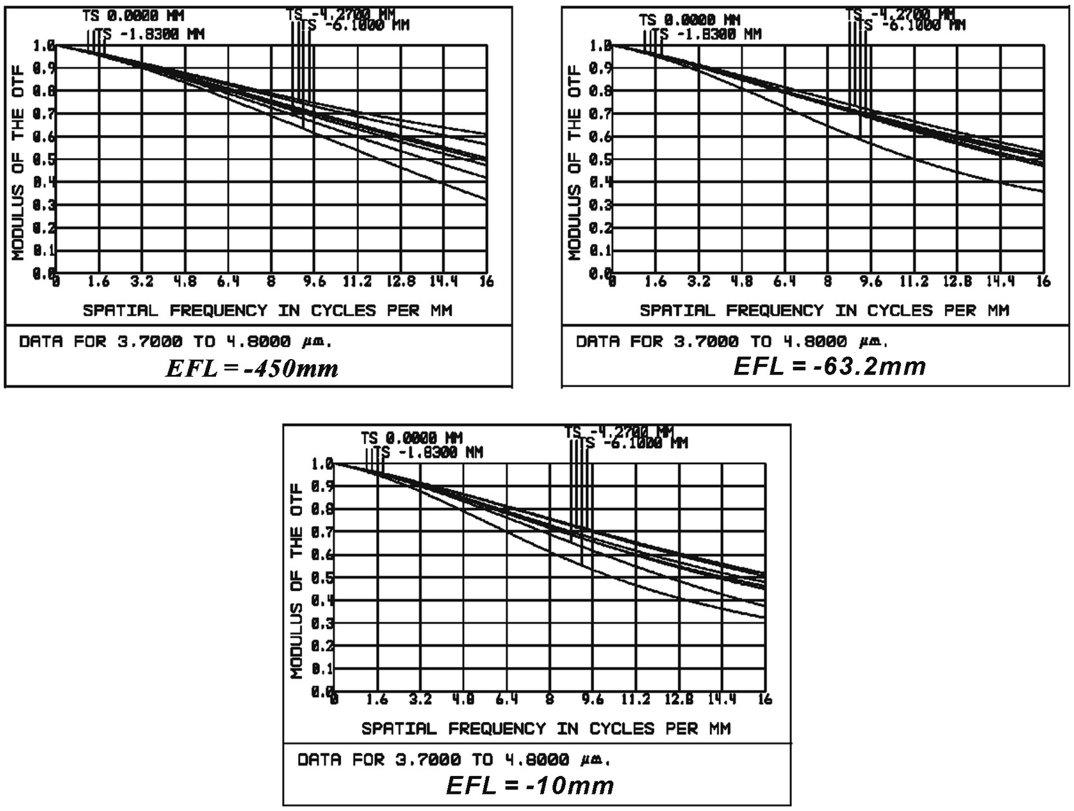

Fig. 6 MTF curves of the system at three zoom positions.

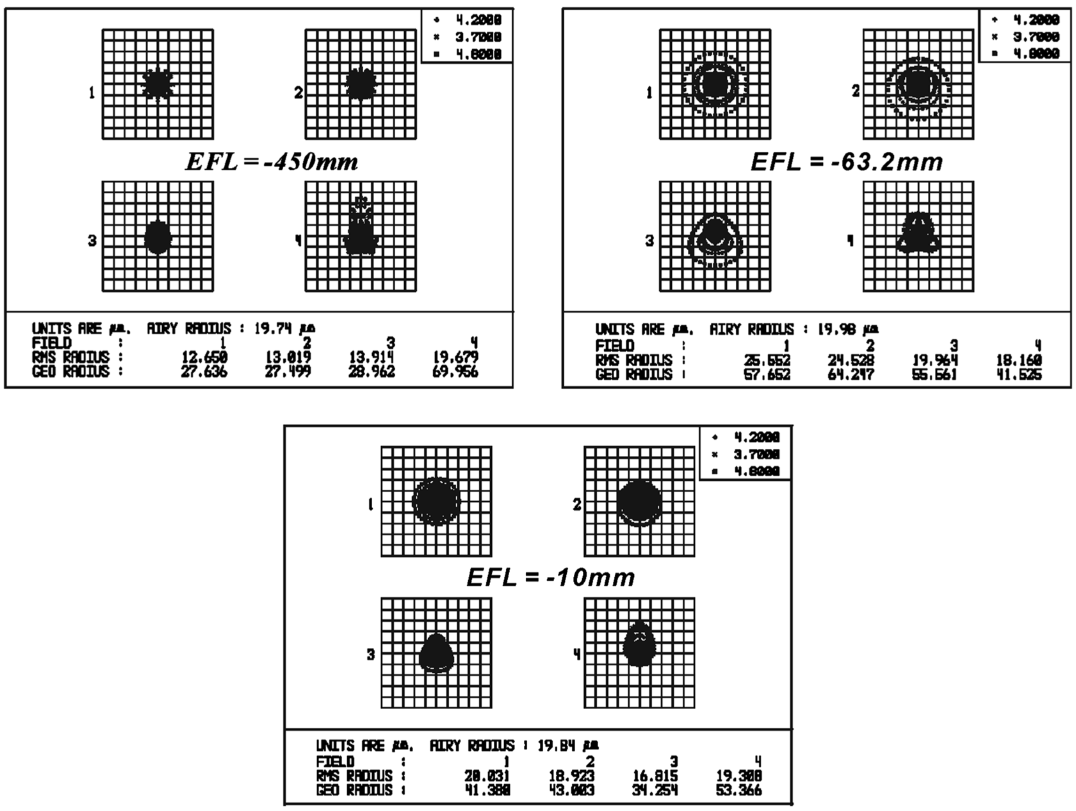

Fig. 7 Spot diagrams of the system at three zoom positions.

4 Conclusions

Using six-component mechanically compensated type, a MWIR zoom system is designed in this paper. The results present this zoom lens achieving good image quality, with specifications of 45 zoom ratio and $F/4$, by utilizing the layout of interlaced mechanical linkage to perform the role of variator and compensator. The six-component mechanically compensated type system can achieve a large zoom ratio with short overall length and moving lengths. The continuous motions of the zoom elements are smooth. Image qualities are good over the entire zoom range. The six-component mechanically compensated type has advantages in the design of MWIR zoom system with a large zoom ratio.

References

1. R. L. Sinclair, "High magnification zoom lenses for 3–5 μm applications," *Proc. SPIE* **3429**, 11–18 (1998).
2. C. W. Kuo, J. M. Miao, and C. H. Tai, "Midwave infrared optical zooming design and kinoform degrading evaluation methods," *Appl. Opt.* **50**(18), 3043–3049 (2011).
3. M. N. Akram, "Design of a multiple-field-of-view optical system for 3- to 5-μm infrared focal-plane arrays," *Opt. Eng.* **42**(6), 1704–1714 (2003).
4. H. S. Kim, C. W. Kim, and S. M. Hong, "Compact mid-wavelength infrared zoom camera with 20:1 zoom range and automatic athermalization," *Opt. Eng.* **41**(7), 1661–1667 (2002).
5. H. S. Kim et al., "Compact MWIR camera with ×20 zoom optics," *Proc. SPIE* **4369**, 673–679 (2001).
6. M. W. Chang, "Design of a compact zoom system for 3–5 micron wave band thermal imager," *Proc. SPIE* **3129**, 144–155 (1997).
7. Z. Y. Fan et al., "Design of high ratio middle infrared continuous zoom optical system," *Proc. SPIE* **8193**, 81931R (2011).
8. M. N. Akram and M. H. Asghar, "Step-zoom dual-field-of-view infrared telescope," *Appl. Opt.* **42**(13), 2312–2316 (2003).
9. Z. D. Xu, X. Liu, and Z. Wei, "Airborne IR system design using 640 × 512 element detector," *J. Nanjing Univ. Aeronaut. Astronaut.* **39**(4), 524–529 (2007).
10. J. Q. Meng, "Dual field zoom (×6) infrared imaging optical system," *Infrared Laser Eng.* **37**(1), 89–92 (2008).
11. L. Zhang, "Optical design for middle infrared zoom system," *J. Appl. Opt.* **27**(1), 32–34 (2006).
12. H. Y. Gao and T. Xiong, "Mid-wavelength infrared dual field-of-view optical system," *Opt. Precision Eng.* **16**(10), 1891–1894 (2008).
13. A. Mann, *Infrared Optics and Zoom Lenses*, SPIE Press, Bellingham, WA (2009).
14. R. G. Li et al., "Design of dual-field-of-view optical system for mid-wave infrared focal-plane arrays," *Laser Infrared* **39**(6), 640–642 (2009).
15. L. J. Chen, P. Li, and L. Ma, "Compact MWIR zoom system," *Infrared Technol.* **32**(10), 562–566 (2010).
16. H. T. Wang and L. X. Guo, "Cooled thermal imaging mid-wavelength infrared zoom camera," *Infrared Technol.* **29**(1), 8–11 (2007).
17. M. C. Sanson and J. Cornell, "MWIR continuous zoom with large zoom range," *Proc. SPIE* **7660**, 76601X (2010).
18. M. C. Sanson et al., "Development of MWIR continuous zoom with large zoom range," *Proc. SPIE* **8012**, 80122F (2011).
19. Y. Aron et al., "Topaz: a novel design of a high magnification, athermalized 1:30 zoom in the MWIR," *Proc. SPIE* **5406**, 97–106 (2004).
20. H. Y. Gao, T. Xiong, and C. C. Yang, "Middle infrared continuous zoom optical system," *Opt. Precision Eng.* **15**(7), 1038–1043 (2007).
21. A. Porta et al., "ERICA: compact MWIR camera with 20× step zoom optics and advanced processing," *Proc. SPIE* **6737**, 673706 (2007).

Zhou Hao received a BS degree in optical information science and technology from Hefei University of Technology in 2009. He is currently pursuing his PhD at the Graduate School of the Chinese Academy of Sciences. His research interests are infrared optical systems and system evaluation.

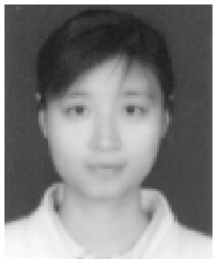

Liu Ying received a PhD degree in optical engineering from Graduate School of the Chinese Academy of Sciences in 2010. She is currently a research assistant at the Changchun Institute of Optics, Fine Mechanics, and Physics, Chinese Academy of Sciences. Her research interests are infrared optical systems and spectrometer.

Sun Qiang received a PhD degree in optical engineering from Nankai University in 2003. He is currently a professor at the Changchun Institute of Optics, Fine Mechanics, and Physics, Chinese Academy of Sciences. His research interests are infrared optical systems and spectrometer.

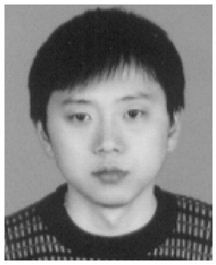

Li Chun received an MS degree in optical engineering from Graduate School of the Chinese Academy of Sciences in 2010. He is currently a research assistant at the Changchun Institute of Optics, Fine Mechanics, and Physics, Chinese Academy of Sciences. His research interests are image enhancement and image fusion.

Zhang Xiaolong received a BS degree in applied physics from Qingdao University of Science and Technology in 2009. He is currently pursuing his PhD at the Graduate School of the Chinese Academy of Sciences. His research interests are optics design and testing.

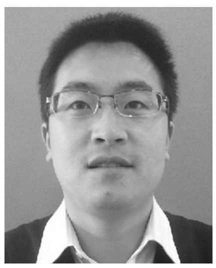

Huang Jianbo received an MS degree in mechanical engineering from Jilin University in 2008. He is currently a research assistant at the Changchun Institute of Optics, Fine Mechanics, and Physics, Chinese Academy of Sciences. His research interests are mechanical system design and testing.